33rd EPS Conference on Plasma Phys. Rome, 19 - 23 June 2006 ECA Vol.**30I**, P-2.187 (2006)

Transport reduction due to sheared $E \times B$ flow in the torsatron TJ-K

M. Ramisch[1)], F. Greiner[2)], N. Mahdizadeh[1)], K. Rahbarnia[1)], U. Stroth[1)]

[1)] *Institut für Plasmaforschung, University Stuttgart, Germany*
[2)] *Institut für Experimentelle und Angewandte Physik, University Kiel, Germany*

Introduction: The understanding of the formation of transport barriers in high-confinement (H-mode) discharges is one of the key objectives in fusion research. Theory considers the decorrelation of turbulent structures by $E \times B$ shear flows as the key process [1]. In particular, the reduction in turbulent transport $\Gamma = < \widetilde{n}\widetilde{v}_r >_t$ could be due to the reduction of the radial correlation length (L_r), which – according to a simple mixing-length estimate – is related to the density fluctuation amplitude $\widetilde{n} = L_r \partial_r n$. $\widetilde{v}_r = \widetilde{E}_\theta / B$ is the fluctuation amplitude of radial $E \times B$-velocity fluctuations. On the other hand, the reduction could also be due to a modification of the phase relation between $\widetilde{n}$ and $\widetilde{v}_r$ [2]. For interchange and ion-temperature-gradient (ITG) driven turbulence it was found that a transport reduction by sheared flows is mostly due to a reduction in the amplitude of turbulent velocity [3]. Other analytical studies suggested, however, that strong shear flows predominantly influence the cross-phase with reduced or in case of collisional drift-waves even locally inward directed transport [4, 5]. Experimental evidence that the cross-phase plays a crucial role in the reduction of turbulent transport is found in a variety of devices amongst others in DIII-D [6], H-1 [7] and TEXTOR [8].

In this work, the influence of shear flows on the spatio-temporal structure of turbulence and radial turbulent transport in the torsatron TJ-K is investigated by means of multi-probe arrays with high spatial resolution. External plasma biasing [9] is applied in order to generate sheared poloidal $E \times B$ flows.

Experimental Setup: TJ-K [10] toroidally confines a low-temperature plasma, which is dimensionally similar to fusion edge plasmas [11]. The major and the minor plasma radius is $R_0 = 0.6$ m and $a = 0.1$ m, respectively. The confining magnetic field has a rotational transform of about $1/3$ with low magnetic shear. TJ-K can be operated with nominal magnetic field strengths in the range $B = 70$–100 mT when electron-cyclotron-resonance heating (ECRH) at 2.45 GHz is used for plasma generation. In the present experiment, the working gas was hydrogen at a neutral gas pressure of $p_0 = 4 \times 10^{-5}$ mbar, a heating power of $P_{\mathrm{ECRH}} = 1.8$ kW and a magnetic field strength of $B = 72$ mT. For these parameters, the typical electron temperature and maximum density is $T_e \approx 7$ eV and $n \approx 2 \times 10^{17}\,\mathrm{m}^{-3}$, respectively. The ions are cold ($T_i < 1$ eV).

As a biasing electrode, a closed stainless steel plate in the shape of the poloidal cross-section of an inner flux surface was used. The electrode with a radial extent of 3 mm and a toroidal extent of 1.5 cm was introduced from a top port into a cross-section with elliptical flux surfaces. Equilibrium-profile and fluctuation measurements have been carried out at outer ports with triangular flux-surface cross-sections. The electrode was biased positively with respect to the grounded vacuum vessel.

For the measurements of turbulent structures in the density fluctuations, two diagnostics consisting of 64 Langmuir probes were used. The first diagnostics is set up on a two-dimensional grid of 8×8 points in the poloidal cross-section on the low-field side and centered at the biased surface. The spatial resolution is 1 cm in vertical and horizontal direction. At all 64 positions, the fluctuations in the ion-saturation current were simultaneously acquired and cross-correlation analyses were carried out on these data. The cross-correlation between each probe of the matrix at a position (R_i, z_j) and one reference probe as a function of a time lag Δt is calculated according to

$$C_{i,j}(\Delta t) = \int \frac{\widetilde{n}_{\mathrm{ref}}(t)}{\sigma_{\mathrm{ref}}} \frac{\widetilde{n}_{i,j}(t+\Delta t)}{\sigma_{i,j}} \mathrm{d}t, \tag{1}$$

where each signal is normalised to its respective rms value σ. In Ref. [12], the probe array and the analysis technique is introduced in more detail. In order to resolve the poloidal structure of turbulence, the matrix has been replaced by a poloidal probe array. The probes are poloidally arranged on a complete circumference of a flux surface near the biased one with a resolution of $\Delta u = 7\,\mathrm{mm}$. For transport measurements, fluctuations in the floating potential and ion-saturation current are acquired each from 32 probes in alternating order, i.e., $\widetilde{v}_{r,i} = -(\widetilde{\phi}_{f,i+1} - \widetilde{\phi}_{f,i-1})/2\Delta u B_i$, where $i = 1, 3, \ldots$ and B_i is calculated. An average cross-phase φ_{vn} between these fluctuations is defined according to [13]

$$\cos(\varphi_{vn}) = \Gamma/\sigma_n \sigma_v. \tag{2}$$

In particular, the local turbulent transport can be expressed in terms of the rms values σ of the fluctuations and the cosine of their cross-phase: $\Gamma = \sigma_n \sigma_v \cos(\varphi_{vn})$. Maximal outward transport is associated with $\varphi_{vn} \approx 0$ and it vanishes for $\varphi_{vn} \to \pi/2$.

Equilibrium profiles: For a bias voltage of $U_b = 100\,\mathrm{V}$, the influence of biasing on the equilibrium is depicted in Fig. 1. The potential inside the biased flux surface is increased leading to a strongly enhanced radial electric field up to the separatrix at $R - R_0 = 13\,\mathrm{cm}$ and, thus, high poloidal $E \times B$ velocities. The potential drop by about 80 V on a distance of 7 cm corresponds to $U_{E\times B} \approx 16\,\mathrm{km/s}$. In the vicinity of the biased surface, the shearing rate $\omega_{E\times B} \approx U'_{E\times B} = \mathrm{d}U_{E\times B}/\mathrm{d}r$ as calculated from the profile of ϕ_f changes from about 100 kHz to maximum values of the order of 1 MHz. In this region, the density gradient steepens by a factor of five, i.e., the gradient scale length L_n decreases. In various experiments, the relative fluctuation level $\Delta n/n$ is observed to stay unchanged or even to decrease. According to the simple mixing-length estimate $\Delta n/n = L_r/L_n$ a reduction in the radial correlation length L_r would be expected.

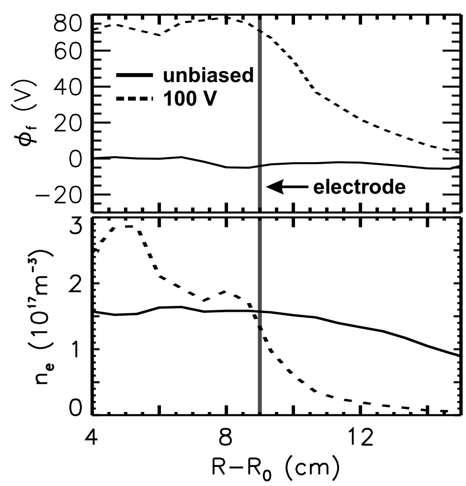

Fig. 1: Increase of the floating potential (top) and steepening of the density gradient (bottom) during biasing.

Turbulent structures: For the unbiased and the biased case ($U_b = 100\,\mathrm{V}$), the spatio-temporal evolution of turbulent density structures is obtained from cross-correlation analyses carried out on the matrix data according to Eq. (1). The results are shown in Fig. 2. In the unbiased case (Fig. 2, top), the structure propagates clockwise into the direction of the electron-diamagnetic drift at a velocity of about 800 m/s. In the biased case, the $E \times B$ velocity becomes dominant and the propagation direction reverses (Fig. 2, bottom). The velocity of the structures is about 15 times larger ($\approx 12\,\mathrm{km/s}$) than in the unbiased case. This is consistent with $U_{E\times B} \approx 16\,\mathrm{km/s}$ as deduced from the ϕ_f profile in Fig. 1 (top), since the diamagnetic velocity, which points into the opposite direction, increases to 4 km/s, i.e., equal to the density gradient by a factor of five. Unexpectedly, the structure becomes larger and even more circular in the biased case. An increase in the correlation lengths from $L_r = 3\,\mathrm{cm}$ and $L_\theta = 2\,\mathrm{cm}$ to 4 cm each is observed at $\Delta t = 0$.

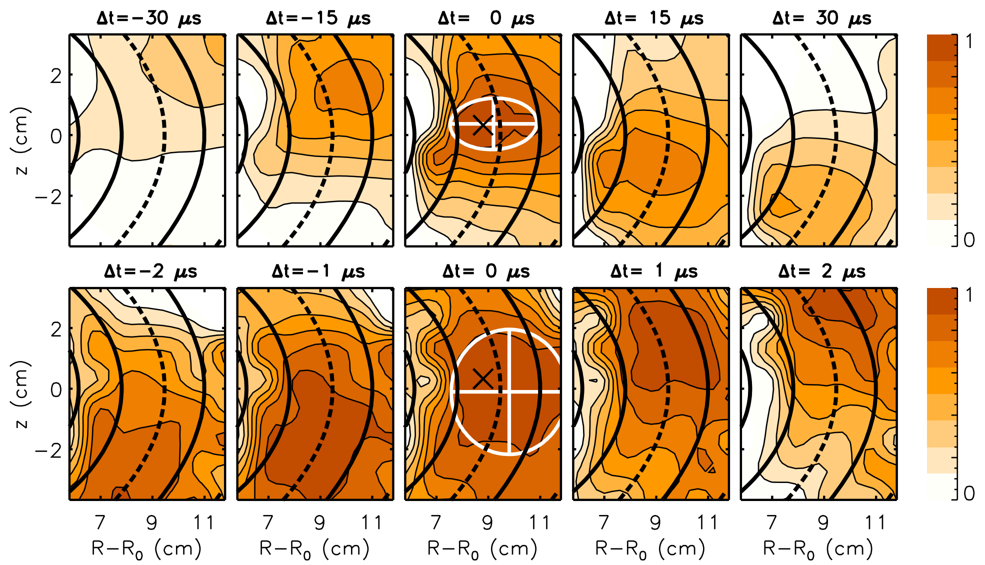

Fig. 2: Contour plots of cross-correlations between matrix probes at five consecutive time lags Δt *for the unbiased (top row) and the biased case (bottom row). At* $\Delta t = 0$ *an ellipse is fitted to contours of 87% correlation.*

A comparison of the structure size at $\Delta t = 0$ to that at $\Delta t = 2\,\mu$s in the biased case reveals a reduction from 4 cm each to $L_r = 3$ cm and $L_\theta = 2$ cm. In the unbiased case, the structure size does not change after $2\,\mu$s, which points to a reduction in the lifetime τ_c during biasing. The same analyses have been carried out on data from the one-dimensional poloidal probe array. On the top of Fig. 3, the poloidal mode structure is shown. Therefor, the cross-correlation between a reference probe and all other probes at $\Delta t = 0$ is averaged over all reference probes on the complete circumference. During biasing, the poloidal mode number changes from $m = 4$ to $m = 3$. For the lifetime, the maximum of the cross-correlations is traced as a function of Δt as long as it stays above a threshold of 0.6. The average over all reference probes is shown in Fig. 3, bottom. During biasing, the lifetime τ_c is reduced by a factor of $1/3$ from 65 to 21 μs.

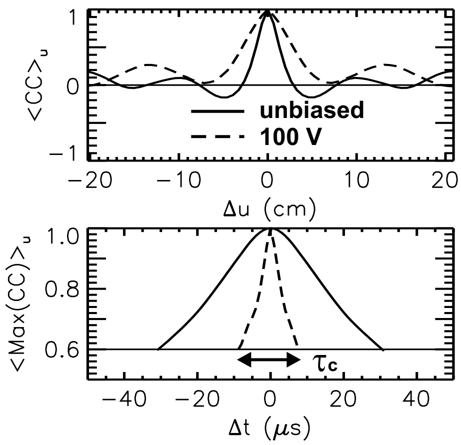

Fig. 3: Average cross-correlation between probes of the poloidal array at $\Delta t = 0$ *(top) and average of the maximum correlation as traced for values larger than 0.6 (bottom).*

Turbulent transport: On the high-field side (HFS), the velocity fluctuations σ_v (Fig. 4a) are halved during biasing. The density fluctuations σ_n are halved on the entire surface (Fig. 4b), whereas σ_v nearly stays unchanged on the low-field side (LFS). On the HFS, the cross-phase φ_{vn} (Fig. 4c) and the radial turbulent transport Γ (Fig. 4d) in general scatter around $\varphi_{vn} = \pi/2$ and 0, respectively. In the unbiased case, the maximum contribution to Γ is found on the LFS as marked by the shaded region. Here, biasing leads to a reduction in Γ by a factor of about $1/4$. With $\sigma_v \approx$const, this might indicate that the contribution of the cross-phase to the reduction in turbulent transport is as important as that of σ_n. Furthermore, Fig. 4d shows that a modification of φ_{vn} can locally lead to enhanced inward transport and, thus, reduce significantly the flux-surface average.

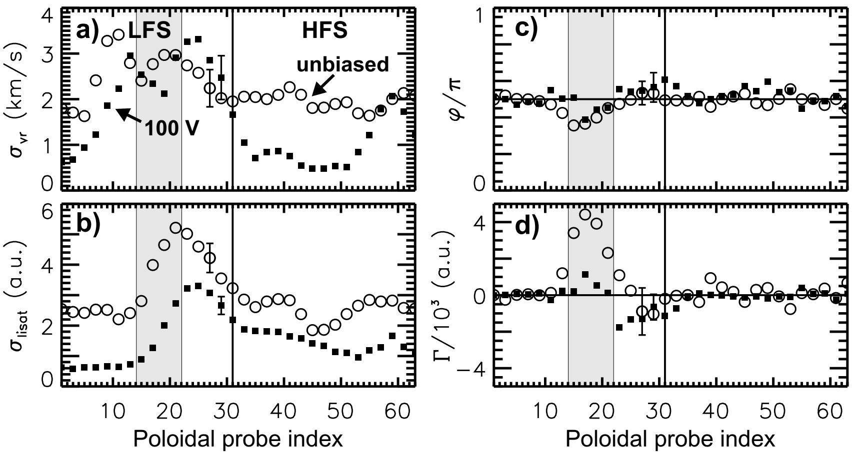

Fig. 4: *Poloidally resolved turbulent transport* Γ *and ingredients. The region of maximum* Γ *is shaded.*

Summary: Plasma biasing was successfully applied to the TJ-K plasma and fields of the order of 1100 V/m have been induced with shearing rates up to 1 MHz, leading to a steepening of the density gradient by a factor of 5 and a reduction in particle transport. At the same time, turbulent density structures on larger spatial scales beyond validity of simple mixing-length estimates remain. However, these structures feature a shortened lifetime of the order of 20 μs. A shortened lifetime would reduce the effective radial step size of a diffusive process. The maximum contribution to the turbulent transport as measured with a poloidal probe array was found on the LFS. In the presence of the $E \times B$ shear flow, the transport on the LFS was reduced due to both, a reduction in density fluctuations and a modification of the cross-phase. For the case of constant fluctuation levels, a reduction solely due to the cross-phase was reported in Ref. [14]. Local measurements on the LFS showed that a substantial fraction of the spectral power was redistributed from the low-frequency range into a high-frequency mode causing inward transport due to cross-phases of $\varphi_{vn} > \pi/2$. Furthermore, the poloidal measurements presented here showed that the particle flux can locally be reversed and, thus, significantly contribute to the reduction in flux-surface averaged transport. Since in TJ-K turbulence is dominated by drift-waves [11], these results are qualitatively consistent with theoretical predictions by Terry *et al.* [4, 5].

References

[1] H. Biglari, P. H. Diamond, P. W. Terry, Phys. Fluids, B **2**, 1 (1990).
[2] K. H. Burrell, Phys. Plasmas **4**, 1499 (1997).
[3] Eun-jin Kim, P. H. Diamond, T. S. Hahm, Phys. Plasmas **11**, 4554 (2004).
[4] P. W. Terry, D. E. Newman, A. S. Ware, Phys. Rev. Lett. **87**, 185001 (2001).
[5] P. W. Terry, D. E. Newman, A. S. Ware, Phys. Plasmas **10**, 1066 (2003).
[6] R. A. Moyer, K. H. Burrell, T. N. Carlstrom *et al.*, Phys. Plasmas **2**, 2397 (1995).
[7] M. G. Shats, D. L. Rudakov, Phys. Rev. Lett. **79**, 2690 (1997).
[8] J. A. Boedo, D. S. Gray, P. W. Terry *et al.*, Nucl. Fusion **42**, 117 (2002).
[9] R. J. Taylor, M. L. Brown, B. D. Fried *et al.*, Phys. Rev. Lett. **63**, 2365 (1989).
[10] N. Krause, C. Lechte, J. Stöber *et al.*, Rev. Sci. Instrum. **73**, 3474 (2002).
[11] U. Stroth, F. Greiner, C. Lechte *et al.*, Phys. Plasmas **11**, 2558 (2004).
[12] M. Ramisch, N. Mahdizadeh, U. Stroth *et al.*, Phys. Plasmas **12**, 032504 (2005).
[13] B. A. Carreras, C. Hidalgo, E. Sánchez *et al.*, Phys. Plasmas **3**, 2664 (1996).
[14] M. Ramisch, F. Greiner, U. Stroth *et al.*, *Proc. 15th Int. Stellarator Workshop, Madrid*, (CIEMAT, Madrid, 2005).